

Full length article

Numerical study of cold-formed steel channel sections under combined web crippling and bending action

Balasubramaniam Janarthanan^a, Mahen Mahendran^{b,*}^a University of Jaffna, Sri Lanka^b Queensland University of Technology, Brisbane, Australia

ARTICLE INFO

Keywords:

Cold-formed steel beams
Web crippling failure
Combined web crippling and bending
Finite element analysis
Design equations

ABSTRACT

Cold-formed steel sections used in floor systems are vulnerable to web crippling, and with increasing span lengths, they are likely to fail under combined web crippling and bending action. A numerical study was therefore undertaken to investigate the combined web crippling-bending interaction behaviour of unlippped channel sections used as bearers in floor systems with fastened supports. Web crippling finite element models developed and validated by the authors in a recent study were extended to investigate the behaviour of unlippped channels under combined action of web crippling and bending while new finite element models were developed for bending and validated using available experimental results. All three types of finite element models were used in a detailed parametric study to obtain the capacities of 12 unlippped channel sections made of G250 and G450 steels under pure and combined web crippling and bending actions. Comparison of the combined web crippling and bending capacities obtained from finite element analyses with the interaction equations in three cold-formed steel design standards, AISI S100, AS/NZS 4600 and Eurocode 3 Part 1.3, showed that the current design equations are accurate for 50 mm bearing length. However, they can also be used to predict the combined web crippling-bending capacities conservatively for bearing lengths of 100 and 150 mm. A new design equation with a suitable capacity reduction factor was then proposed to improve the accuracy of predicting the mid-span load capacity of channel sections subject to combined web crippling and bending actions.

1. Introduction

Cold-formed steel sections are increasingly used as bearers in floor systems due to their lightweight and structural efficiency. Unlippped channel sections are one of the conventional cold-formed steel sections commonly used as bearers in floor systems. These channel sections are available in thicknesses up to 8 mm due to the use of advanced cold-forming technology [1]. Fig. 1 shows the typical unlippped channel sections while Table 1 lists their nominal dimensions. These cold-formed steel sections are vulnerable to web crippling at the points of concentrated loads or supports due to their high width to thickness ratio. They are also subjected to higher bending stresses in addition to web crippling with increasing spans. This will reduce the ultimate capacity of channel section bearers, making it more critical in design. However, no research has yet been undertaken to investigate the reduced capacity of cold-formed unlippped channel section bearers with fastened supports under combined web crippling and bending actions.

The AISI standard web crippling test method [2] groups web

crippling failure under four cases such as End-One-Flange (EOF), Interior-One-Flange (IOF), End-Two-Flange (ETF) and Interior-Two-Flange (ITF) based on loading conditions and failure region as shown in Fig. 2. Among them, cold-formed steel beams under Interior-One-Flange (IOF) load case are subjected to combined web crippling and bending actions with increasing span lengths. Theoretical web crippling investigations are complicated because of the presence of non-uniform stress distribution under applied load, local yielding at the loaded area, bending caused by eccentric loading, inelastic behaviour of the web element with initial imperfections and different web-flange restraint levels [3]. Therefore, theoretical analysis of web crippling-bending interaction behaviour is even more complicated. Also, experimental investigations of web crippling-bending interaction are expensive and time consuming as these experiments require long specimens. Since the authors have previously conducted web crippling investigations of unlippped channel sections, an effective solution for web crippling-bending interaction investigation is to use numerical analysis based on finite element models that have been validated using the

* Corresponding author.

E-mail address: m.mahendran@qut.edu.au (M. Mahendran).

results of experimental studies performed in the case of web crippling.

Current cold-formed steel sections such as North American Specification (AISI S100) [4], Australian/New Zealand standard (AS/NZS 4600) [5] and Eurocode 3 Part 1–3 (ECS, 2006) [6] use different web crippling-bending interaction equations, which were developed using different experimental test set-ups and procedures [7–10]. Both North American Specification (AISI S100) [4] and Australian/New Zealand standard (AS/NZS 4600) [5] use different coefficients to determine the web crippling capacities for fastened and unfastened support conditions. Recently conducted IOF test results of Gunalan and Mahendran [11] and Janarthanan et al. [12] showed that web crippling capacity was increased by 10–15% for unlippped channel sections when their flanges were fastened to their supports. Similar web crippling capacity enhancement was observed for rectangular hollow flange steel beams by Keerthan et al. [13] and Steau et al. [14]. Also, different web crippling failure modes were observed for unfastened and fastened support conditions as shown in Fig. 3. Hence the effects of fastened support conditions should also be investigated for unlippped channel sections under combined web crippling and bending actions.

This paper presents the details of a numerical investigation on the structural behaviour of unlippped channel section bearers under combined web crippling and bending actions. As commonly used in practice, channel sections were considered to have their flanges fastened to the supports. The web crippling finite element model developed and validated previously by the authors [15] was extended to include the effects of combined actions of web crippling and bending while a new finite element model was developed for bending action and validated using the available experimental results of Young and Hancock [10]. These finite element models were then used in a detailed parametric study of 12 unlippped channel section bearers made of two steel grades (G250 and G450). Using the parametric study results, the accuracy of web crippling-bending interaction equations given in three cold-formed steel standards was assessed, and improved design equations are proposed.

2. Review of relevant literature and current design equations

This section briefly reviews the relevant past studies on cold-formed steel sections under combined web crippling and bending actions and discusses the currently available design equations. Baehre [7] first observed the reduction in web crippling capacity of corrugated sheets due to the presence of bending and developed a web crippling-bending capacity interaction equation. Ratliff [8] investigated the web

Table 1
Nominal dimensions of unlippped channel sections [1].

Section	d (mm)	b _f (mm)	t (mm)	f _y (MPa)	f _u (MPa)	r _i (mm)	w (kg/m)
300 × 90	300	90	8.0	400	450	8	28.5
× 8.0							
300 × 90	300	90	7.0			8	25.1
× 7.0							
300 × 90	300	90	6.0	450	500	8	21.6
× 6.0							
250 × 90	250	90	6.0			8	19.2
× 6.0							
230 × 75	230	75	6.0			8	16.9
× 6.0							
200 × 75	200	75	6.0			8	15.5
× 6.0							
200 × 75	200	75	4.7			4	12.4
× 5.0							
180 × 75	180	75	4.7			4	11.6
× 5.0							
150 × 75	150	75	4.7			4	10.5
× 5.0							
125 × 65	125	65	3.8			4	7.23
× 4.0							
100 × 50	100	50	3.8			4	5.59
× 4.0							
75 × 40	75	40	3.8			4	4.25
× 4.0							

Note: d – section depth, b_f – flange width, t – nominal thickness, f_y – minimum yield strength, f_u – minimum tensile strength, r_i – inside corner radius, w – unit weight per unit length.

crippling-bending interaction behaviour of lipped channel sections using a test set-up with mid-span loading in which the web of lipped channel sections was connected to steel brackets at the ends while the bottom flange was connected to 12.7 mm plywood using screws at 30.5 mm spacing (Fig. 4). The interior support was unrestrained in some tests while both web and compression flange were restrained using web stiffeners in other tests. Two different equations were proposed for channel sections with and without web stiffeners.

Hetrakul and Yu [9] performed an experimental investigation using 38 channel sections with thickness less than 3 mm with unfastened supports. Their test set-up included two similar channel sections facing each other in a box beam arrangement, which is similar to the recently

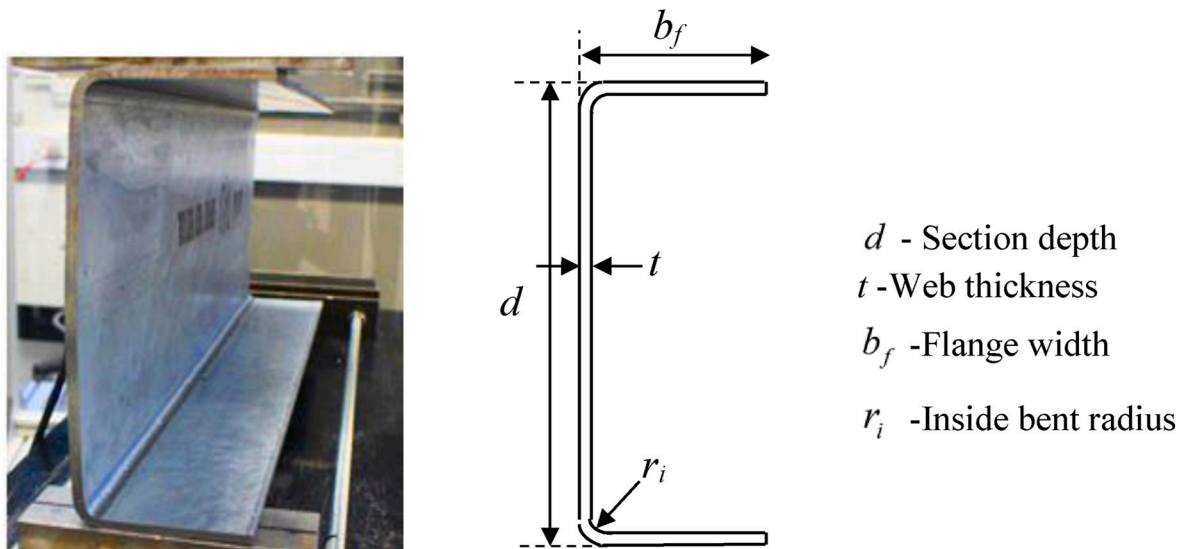


Fig. 1. Unlippped channel section.

updated AISI web crippling standard method [2] with increased specimen lengths. They proposed a web crippling-bending interaction equation, which is still used in AS/NZS 4600 [5]. However, their equation is only applicable to the following ranges: $44 < d_1/t < 200$, $r_i/t < 3$, $12 < l_b/t < 65$, $225 < f_y < 380$ MPa $1.16 < t < 1.65$ mm, where d_1 , r_i , l_b , t and f_y are the clear web depth, inside bent radius, bearing length, thickness and yield strength of the sections.

Young and Hancock [10] investigated the combined web crippling and bending behaviour of thicker (4–6 mm) cold-formed unlippped channel sections with unfastened flange supports. They used back to back channel sections with their webs connected to the support plates at the specimen ends as shown in Fig. 5, and the load was applied at mid-span. This test set-up is different to that of Hetrakul and Yu [9]. Ren et al. [16] developed finite element models using ANSYS based on Young and Hancock’s [10] test set-up and their numerical parametric study results showed that the then North American Specification [17] was conservative for channel sections with web slenderness ranging from 7.8 to 108.5.

Soliman et al. [18] numerically investigated the interaction behaviour of web crippling and bending of thin unlippped channel sections after validating their FE models based on Young and Hancock’s [10] test data. Based on their results, the design equations in the then North American, Australian/New Zealand, British and Egyptian cold-formed steel specifications [19–22] were found to be mostly inadequate for web crippling under IOF load case. They also reported that the interaction design equations in both Australian/New Zealand and British standards [20,21] are generally inadequate while those in the North American and Egyptian Standards [19,22] are adequate for their study range. However, their findings cannot be compared with those from recent or current studies since those design equations have now been modified and improved.

As seen in the above review, only a few experimental and finite element studies have been undertaken in this area. Importantly, the test

set-ups used in the experimental studies are different. The three major cold-formed steel design standards, North American Specification (AISI S100) [4], Australian/New Zealand standard (AS/NZS 4600) [5] and Eurocode 3 Part 1.3 [6] use three different combined web crippling-bending interaction equations, but the accuracy of their capacity predictions has not been adequately evaluated. As shown in Fig. 6, all three interaction equations are based on the pure web crippling (P_n) and bending (M_n) capacities of channel sections. Details of the three interaction equations are given next.

Both AISI S100 [4] and AS/NZS 4600 [5] use the same unified web crippling design equation (Equation (1)) with the same IOF web crippling coefficients. The IOF coefficients are only available for unfastened supports and not for fastened supports. Table 2 gives the coefficients proposed by Janarthanan et al. [15] for unlippped channel sections with fastened supports and the coefficients in AISI S100 [4] for unfastened supports. Both Standards also use the same procedure to determine the bending capacity. However, they use different web crippling-bending interaction equations as shown in Equations (2) and (3).

$$R_b = C_r^2 f_y \sin \theta \left(1 - C_w \sqrt{\frac{d_1}{t}}\right) \left(1 - C_r \sqrt{\frac{r_i}{t}}\right) \left(1 + C_l \sqrt{\frac{l_b}{t}}\right) \quad (1)$$

$$\text{AISI S100 } 0.91 \left(\frac{P}{P_n}\right) + \left(\frac{M}{M_n}\right) \leq 1.33 \quad (2)$$

$$\text{AS/NZS 4600 } 1.07 \left(\frac{P}{P_n}\right) + \left(\frac{M}{M_n}\right) \leq 1.42 \quad (3)$$

where d_1 - clear web height of channel section. l_b - bearing length, r_i - inside corner radius, t - section thickness, f_y - material yield strength, C , C_r , C_l and C_w - web crippling coefficients, P - Design concentrated load or reaction in the presence of bending moment, P_n or R_b - Nominal capacity

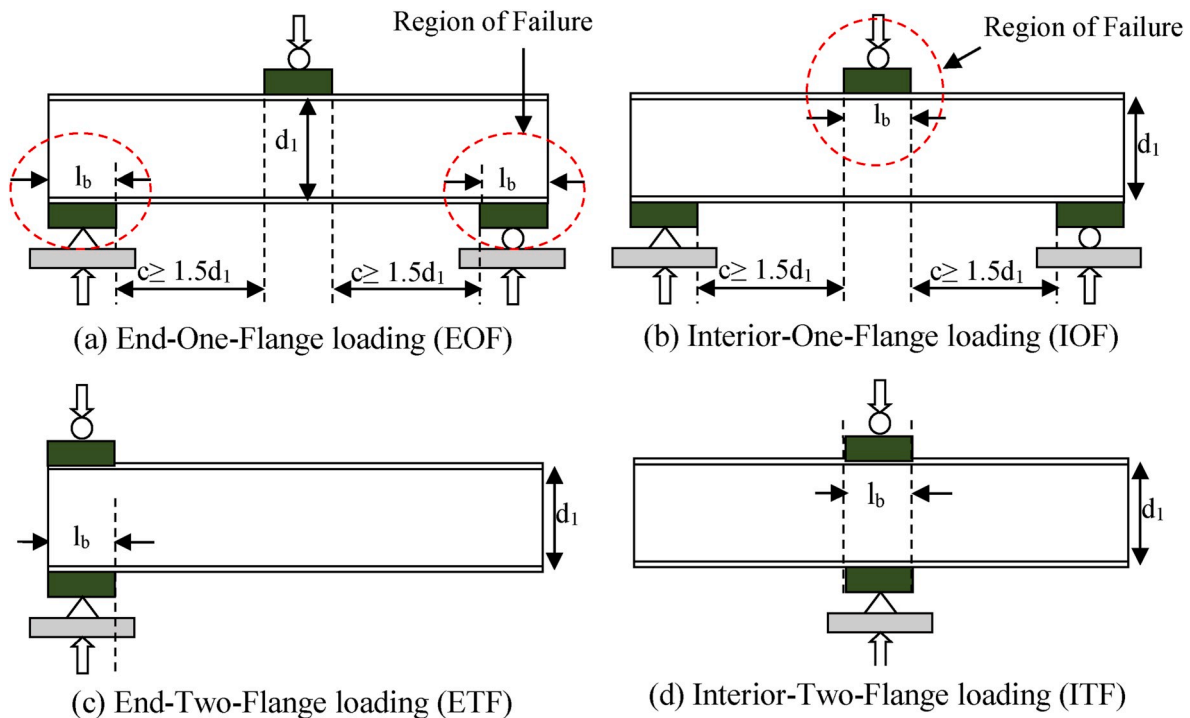
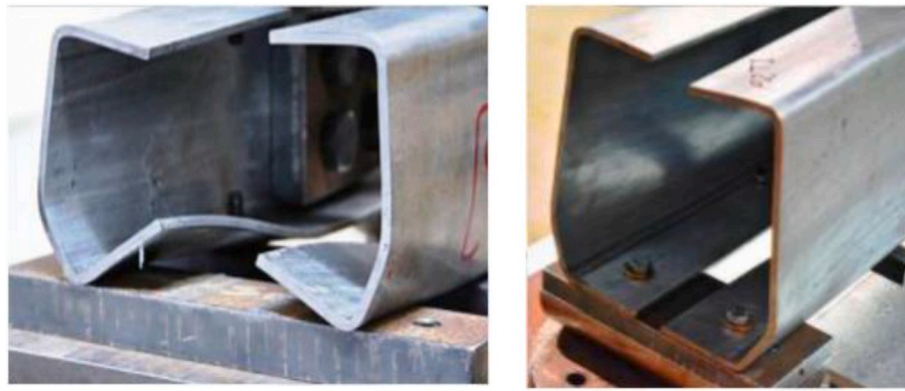


Fig. 2. Load cases for web crippling tests [2].



(a) Unfastened supports [11]

(a) Fastened supports [12]

Fig. 3. Effects of support conditions on the web crippling failure mode.

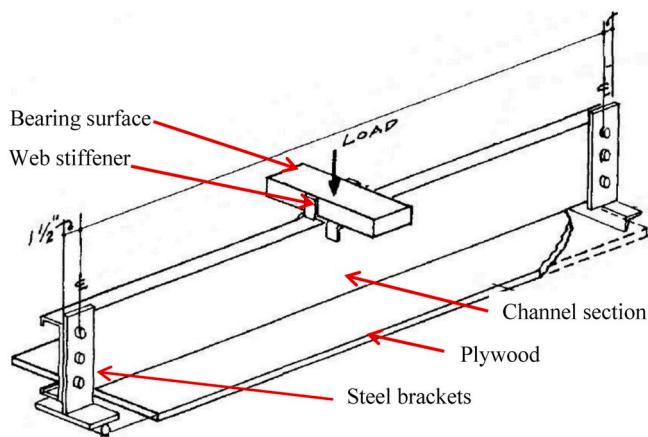
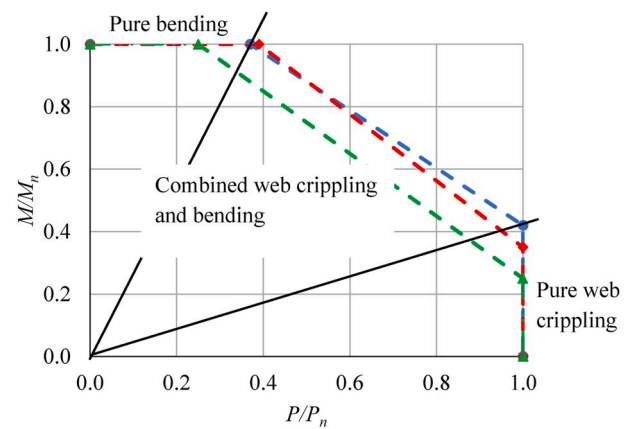


Fig. 4. Combined web crippling-bending test set-up used by Ratliff [8].



—●— AISI S100 - - - AS/ NZS4600 - - - Eurocode-3 Part 1-3

Fig. 6. Web crippling-bending interaction equations.

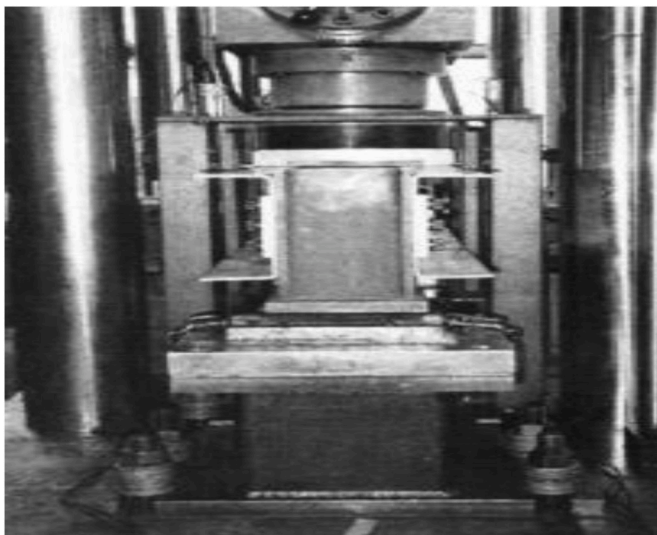


Fig. 5. Combined web crippling-bending test set-up used by Young and Hancock [10].

for concentrated load or reaction, M - Design bending moment at, or immediately adjacent to, the point of application of the design concentrated load (P) or reaction (R^*) and M_n - Nominal section moment capacity.

Table 2

Web crippling coefficients for unlippped channel sections.

Support condition	C	C_r	C_l	C_w
Unfastened (AISI S100) [4]	20.5	0.17	0.11	0.001
Fastened (Janarthanan et al. [15])	4.6	0.23	0.52	0.001

Eurocode 3 Part 1–3 [6] uses different web crippling design equations for different load cases without distinguishing between fastened and unfastened support conditions. Two web crippling equations (Equations (4) and (5)) are used in Eurocode 3 Part 1–3 to determine the IOF web crippling capacity depending on the bearing length to thickness ratio (l_b/t). Equation (6) is recommended for web crippling-bending interaction, where all parameters are the same as defined for Equation (2).

$$\text{if } l_b / t \leq 60 P_n = \frac{k_3 k_4 k_5 \left[14.7 - \frac{l_b/t}{49.5} \right] \left[1 + 0.007 \frac{l_b}{t} \right] t^2 f_y}{\gamma_{M1}} \quad (4)$$

$$\text{if } l_b / t > 60 P_n = \frac{k_3 k_4 k_5 \left[14.7 - \frac{l_b/t}{49.5} \right] \left[0.75 + 0.011 \frac{l_b}{t} \right] t^2 f_y}{\gamma_{M1}} \quad (5)$$

$$\frac{P}{P_n} + \frac{M}{M_n} \leq 1.25 \quad (6)$$

where h_w is the web height between the midlines of the flanges, γ_{M1} is the material safety factor, and k_3 , k_4 and k_5 are the coefficients for flange-web angle, material yield strength and inside corner radius to thickness ratio.

3. Development and validation of finite element models

3.1. Web crippling

Web crippling capacities of unlippped channel sections should be known prior to investigate their behaviour under combined action of web crippling and bending. Authors have recently completed detailed experimental and numerical studies of the web crippling capacities of unlippped channel sections with their flanges fastened to supports [12, 15]. Their web crippling capacity results will be used in this study while their finite element (FE) model will be extended to include the effects of combined web crippling and bending actions. Hence this section first presents the important results of their work including the details of FE models.

Janarthanan et al.'s [12] test set-up based on the new AISI standard web crippling test guidelines [2] was made of two identical unlippped channel sections facing each other in a box beam arrangement, where the two unlippped channel sections were connected via the top and bottom flanges at quarter points along the length as shown in Fig. 7. Test specimen lengths were chosen as $3d+3l_b$, where d is the overall channel section depth and l_b is the bearing length. Finite element models of the tested unlippped channels were developed and validated using test results [15].

Janarthanan et al. [15] developed full and simplified FE models to investigate the effects of test set-up on the web crippling capacity (Fig. 8). Full FE model consisted of 14 contacts and tie connections whereas simplified FE model only consisted of 3 contacts and tie connections. The comparison of web crippling capacity results from the two models showed that the difference was only 2.4% (higher for full models). However, full FE models require more computational resources compared to simplified FE models due to more involved contacts. Therefore, simplified FE models were used in their parametric studies. In their model, S4R elements were used after investigating the effects of S4, S4R, S4RS and S4RSW shell elements. The 5×5 mm mesh was used at the webs and flanges of channel sections whereas 5×0.5 mm fine mesh was used at the corners to ensure proper load transfer from flanges to web of the channel sections. The mechanical properties of steel were measured using tensile coupon tests [23] and were assigned in ABAQUS/CAE using two material models such as perfect plastic and multilinear material models [24,25]. The difference in the ultimate web crippling capacities was only 2.8% when strain hardening was included.

Therefore, simplified material model was used in their web crippling parametric study.

Fig. 9 shows the boundary conditions of simplified models. In the FE model, the displacements (x and y) of the support plates were restrained except in the longitudinal direction of the specimen (z direction). The displacements (x and z) of the loading plate were restrained except in the vertical direction. The vertical displacement of the loading plate was assigned as 20 mm, and the displacement rate was controlled using the Amplitude function, available in ABAQUS [24]. The 8 mm holes on the flanges of sections were fixed in the x-direction to simulate the lateral restraint effects of angles, instead of explicitly modelling the angles. The support and loading plates were allowed to rotate about their x-axis only (axis parallel to the flanges of sections) to simulate half round supports. The two 10 mm thick web side plates used at the supports were simulated by increasing the thickness of 100 mm width partitioned web to $20+t_w$, where t_w is the web thickness.

Janarthanan et al. [15] conducted a parametric study by considering 12 commercially available channel sections made of two steel grades subjected to concentrated load via three bearing lengths of 50, 100 and 150 mm. Table 3 presents the results obtained from this numerical parametric study. All of these web crippling capacity results will be used in this study on combined web crippling and bending actions. Their simplified web crippling FE model, validated using test results, will be used here by increasing the span lengths to simulate the behaviour of unlippped channel sections subject to combined bending and web crippling actions.

3.2. Bending

Bending capacity of unlippped channel sections should also be known prior to investigating their behaviour under combined web crippling and bending action. Therefore, FE models were developed and analysed to investigate the behaviour of unlippped channel sections in bending and to determine their bending capacities. For validation purposes, FE models were first developed to simulate Young and Hancock's [10] bending tests. In their tests, cold-formed steel unlippped channel sections with nominal depths in the range of 75–300 mm, flange widths in the range of 40–90 mm and nominal thicknesses in the range of 4–6 mm were used as seen in Table 4. Table 5 presents the mechanical properties of each section reported by Young and Hancock [10], which are used as input to the FE models for validation purposes.

Young and Hancock's [10] bending test set-up consisted of two similar channel sections with a length of 1270 mm, placed back to back and their webs were connected to the support and loading blocks as shown in Fig. 10. The distance between the loading and support points was 350 mm while the distance between the two loading points was 480 mm. A hinge support condition was used at one end support using a half

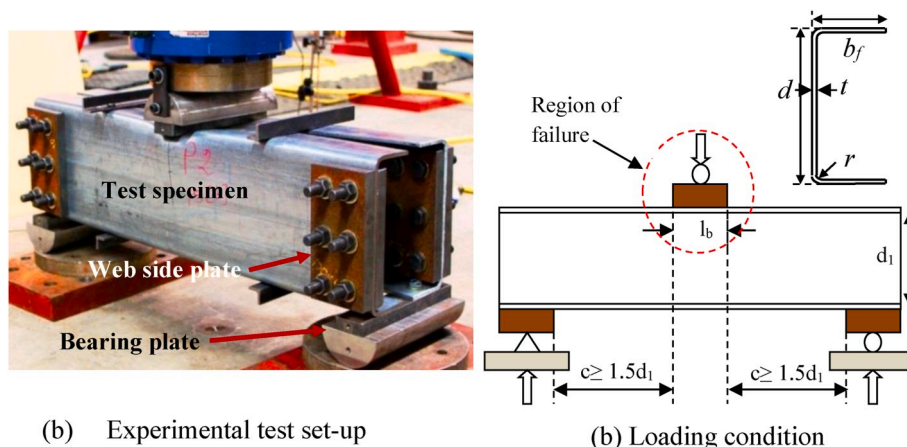


Fig. 7. Web crippling test set-up used by Janarthanan et al. [12].

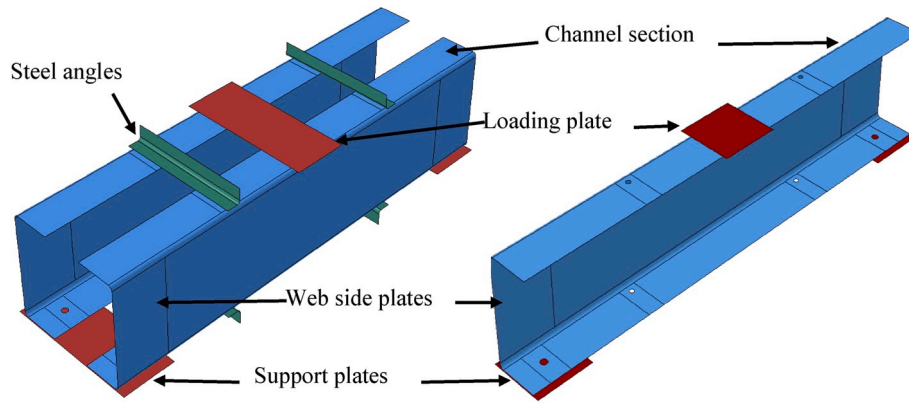


Fig. 8. Web crippling FE models used by Janarthanan et al. [15].

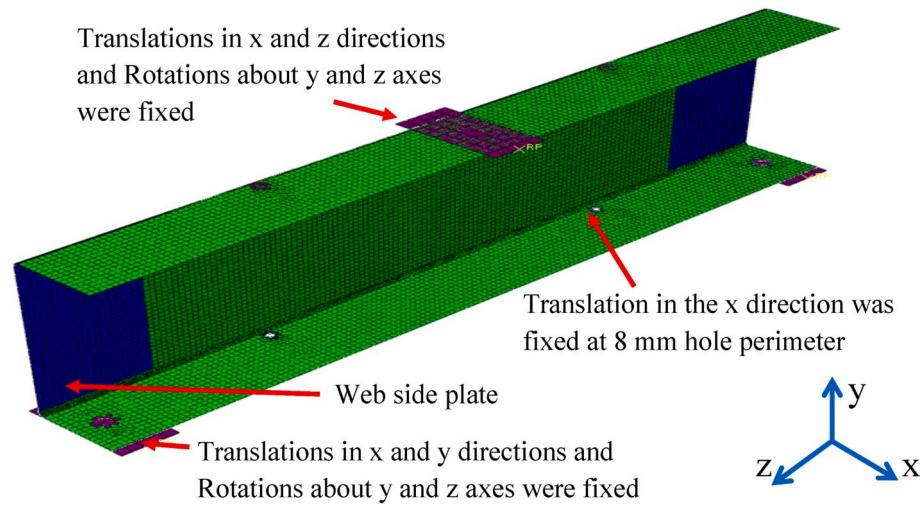


Fig. 9. Boundary conditions of the simplified web crippling FE model [15].

round while a roller support condition was used at the other end support and two loading points using half rounds and Teflon papers. The load was applied via the two loading points using a displacement control method at a rate of 0.8 mm/min. The failure load was obtained from the tests and the corresponding moment for each channel section was determined by multiplying a quarter of the applied load at failure by the distance from the support to the loading point. Table 4 gives the ultimate bending moment capacities obtained from their tests.

This tests data was used to validate the FE models developed in this study using ABAQUS/CAE. In these FE models, unlippped channel sections subject to bending were modelled using S4R shell elements while loading plates were modelled using R3D4 rigid elements. Support and loading plates were developed using contacts and tie connections as shown in Fig. 11. In the developed FE model, a hinge support was used at one end support by restraining the displacements in x, y and z directions and rotations about y and z-axes similar to the test set-up. The boundary conditions similar to the hinge support, but with a z-axis movement released were used at the other end support to simulate the roller support. The x-axis displacement and the y and z-axes rotations were restrained at the two loading points. The vertical deflection of the loading points was assigned as 50 mm in the initial stage of analyses, and the displacement rate was controlled using the Amplitude function, available in ABAQUS.

The developed FE models were analysed using static general and quasi-static analysis based on explicit integration scheme [24–26]. The developed FE models of unlippped channel sections in bending were validated in terms of their ultimate bending capacities and behaviour.

The ultimate bending moment capacities from the developed FE models using two different analysis methods are compared with Young and Hancock's [10] test results in Table 6. The results show that the prediction accuracy is good and it is higher for the FE models using explicit analysis with the mean and COV values of 0.99 and 0.04 compared to static general analysis. Therefore, the developed FE models with explicit analysis were used in a parametric study in this research. Fig. 12 shows the failure modes of unlippped channels in bending as predicted by FEA. Further details of FE modelling including the details of explicit and static general analyses are given in Ref. [15].

4. Channel sections subject to combined web crippling and bending actions

The FE model of unlippped channel section subject to combined web crippling and bending action is similar to that for web crippling action, but with an increased span length. Therefore, the web crippling FE model of unlippped channel section with a mid-span load and the boundary conditions as shown in Fig. 9 was adopted in the study on combined web crippling and bending action. The span lengths of FE models for combined web crippling and bending action were determined using Equation (7), which was suggested by Zhao and Hancock [27] for square hollow sections. Young and Hancock [10] and Ren et al. [16] also used this equation to determine the span length of specimens in their combined web crippling and bending tests of unlippped channel sections with unfastened supports. This equation is based on the maximum bending moment ($M = PL/4$) for simply supported sections subject to a

Table 3
Web crippling capacities of unlippped channel sections with fastened supports [15].

Section	Bearing Length (l_b)					
	$l_b = 50$ mm		$l_b = 100$ mm		$l_b = 150$ mm	
	$f_y = 450$ MPa	$f_y = 250$ MPa	$f_y = 450$ MPa	$f_y = 250$ MPa	$f_y = 450$ MPa	$f_y = 250$ MPa
100 × 51	11.2	7.2	13.5	8.3	15.3	9.8
× 1.5						
100 × 50	56.4	34.2	72.2	43.8	71.8	44.2
× 4.0						
125 × 65	56.1	35.8	75.5	46.0	84.4	53.6
× 4.0						
150 × 64	11.9	7.6	13.9	8.4	15.5	10.1
× 1.5						
150 × 75	84.6	52.8	112.0	66.9	131.2	80.2
× 5.0						
180 × 75	85.8	53.7	109.0	65.5	132.2	81.2
× 5.0						
200 × 76	11.5	7.5	14.1	8.6	15.5	10.3
× 1.5						
200 × 76	25.8	16.4	33.6	20.0	37.9	24.3
× 2.4						
200 × 75	86.1	54.1	109.8	67.5	133.2	81.9
× 5.0						
230 × 75	140.0	84.9	167.1	99.5	196.6	117.6
× 6.0						
250 × 90	142.0	85.8	150.4	91.2	173.5	102.9
× 6.0						
300 × 90	142.0	87.3	151.8	92.8	174.3	103.7
× 6.0						

Table 4
Bending moment capacities of unlippped channel sections [10].

Section	d (mm)	b_f (mm)	t (mm)	r_i (mm)	L (mm)	M_{Exp} (kNm)
75 × 40 × 4-a	74.4	40.3	3.84	3.9	1268.0	6.44
75 × 40 × 4-b	74.4	40.2	3.85	3.9	1267.8	
100 × 50 × 4-a	99.2	50.3	3.83	4.1	1269.9	11.64
100 × 50 × 4-b	99.2	50.4	3.83	4.1	1269.2	
125 × 65 × 4-a	124.9	65.5	3.84	3.9	1269.2	16.20
125 × 65 × 4-b	124.9	65.5	3.83	3.9	1269.1	
200 × 75 × 5-a	198.8	75.9	4.70	4.2	1272.4	40.48
200 × 75 × 5-b	198.8	75.9	4.69	4.2	1271.3	
250 × 90 × 6-a	249.5	90.1	6.01	7.9	1269.2	79.90
250 × 90 × 6-b	249.3	90.0	6.00	7.9	1269.7	
300 × 90 × 6-a	298.5	91.2	6.00	8.4	1269.8	92.89
300 × 90 × 6-b	298.8	91.2	6.00	8.4	1271.5	

Note: d – section depth, b_f – flange width, t – measured thickness, r_i – inside corner radius, L – length, Ultimate moment M_{Exp} .

concentrated mid-span load. The factor k was included in the equation to determine the level of interaction between bending moment and concentrated load. The k factors chosen were 0.50, 0.75, 1.00 and 1.25 for all the unlippped channel sections. The span length L depends on the k factor chosen and the web crippling (P_n) and bending (M_n) capacities of the considered channel section, which were determined using the developed and validated FE models as discussed in the previous sections (Sections 3.1 and 3.2).

Table 5
Mechanical properties of channel sections tested in bending [10].

Section	Nominal f_y (MPa)	Measured		
		f_y (MPa)	f_u (MPa)	ϵ_u (%)
75 × 40 × 4.0	450	450	525	20
100 × 50 × 4.0	450	440	545	20
125 × 65 × 4.0	450	405	510	23
200 × 75 × 5.0	450	415	520	24
250 × 90 × 6.0	450	445	530	21
300 × 90 × 6.0	450	435	535	23

$$\text{Span length } (L) = 4k \frac{M_n}{P_n} \tag{7}$$

The failure of shorter channel sections is dominated by web crippling while the failure of longer channel sections is dominated by bending under the combined action of web crippling and bending. Twelve unlippped channel sections shown in Table 3 were considered in the parametric study for web crippling in the authors’ previous research [15]. The same sections were chosen with three different bearing lengths of 50, 100 and 150 mm for this study. Since the span length depends on the web crippling and bending capacities, it varied for each channel section depending on the bearing length. Hence, Python script was used to generate all the FE models required in this study.

In this FE model, S4R elements were used for deformable shell channel sections while R3D4 elements were used for rigid support and loading plates. The mesh size was chosen as 5 mm × 5 mm for the web and flange elements while a finer mesh size of 5 mm × 0.5 mm was used at the corner region of channel section models. Two steel grades, G250 and G450 were considered and the nominal material yield strength (250 or 450 MPa) was simulated using an elastic perfect plastic material model. Quasi-static analyses of the developed FE models were undertaken based on explicit dynamics, to avoid convergence difficulties involved in static general analysis. A mass scale of 10 was used with thin channel sections (up to 4.7 mm) while a value of 100 was used with thick channel sections to enhance the speed of the analysis. The mid-span concentrated load at failure and the corresponding bending moment at mid-span were obtained from FEA and are given in Tables 7–9, for bearing lengths of 50, 100 and 150 mm, respectively.

Fig. 13(a) and (b) show the ultimate failure modes of Grade 450 180 × 75 × 5 mm channel sections subject to a concentrated load at mid-span via a bearing length of 50 mm with varying span lengths (k values of 0.50 and 1.25). The failure was observed in the web and top flange of channel sections for short span length channel with a k value of 0.50 as shown in Fig. 13 (a) while yielding was mostly observed near the corners and flanges of channel sections with a k value of 1.25 as shown in Fig. 13 (b). This shows that web crippling is dominant in the short channel sections while bending is dominant in the long channel sections.

5. Comparison with current design equations

The results obtained from the FEA based parametric study of 12 unlippped channel sections with four span lengths ($k0.50, k0.75, k1.00$ and $k1.25$) and three bearing lengths (50, 100 and 150 mm) were plotted as shown in Fig. 14 and compared with the combined web crippling and bending interaction equations provided in AS/NZS 4600, AISI S100 and Eurocode 3 Part 1.3. A similar pattern was observed in Ren et al.’s [16] finite element analysis results.

As seen in Fig. 14, AISI S100 [4] and AS/NZS 4600 [5] interaction equations predicted the capacities of channel sections subject to a mid-span concentrated load via 50 mm bearing length reasonably well while Eurocode 3 Part 1.3 [6] underestimated the capacity under combined web crippling and bending actions. The interaction equations in all three cold-formed steel standards underestimated the combined capacity of channel sections subject to a mid-span concentrated load via

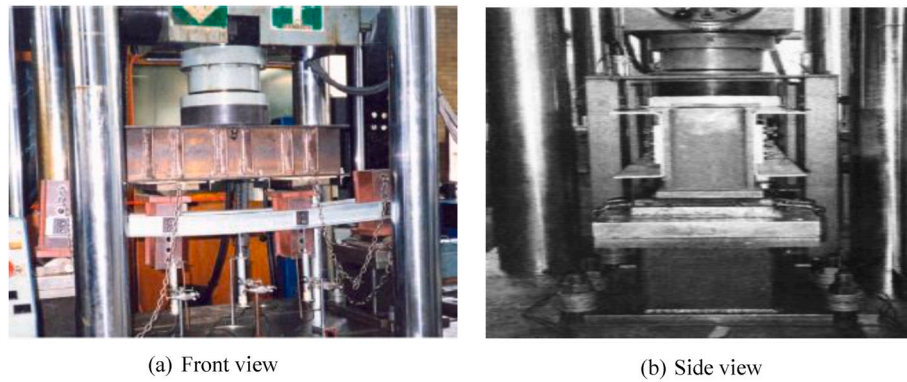


Fig. 10. Bending test set-up used by Young and Hancock [10].

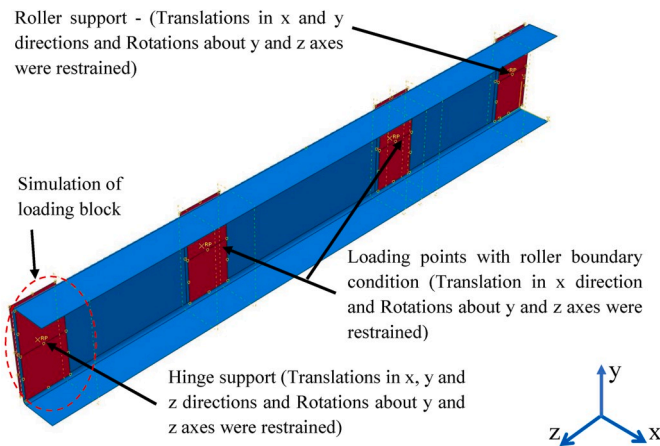


Fig. 11. FE model of unlippped channel in bending.

Table 6
Comparison of bending moment capacities from tests and FEA in kNm.

Section	Test	Static general	FEA/ Test	Explicit MS100	FEA/ Test
75 × 40 × 4.0	6.44	6.28	0.98	6.28	0.98
100 × 50 × 4.0	11.64	10.72	0.92	10.74	0.92
125 × 65 × 4.0	16.20	15.49	0.96	15.84	0.98
200 × 75 × 5.0	40.48	42.08	1.04	40.11	0.99
250 × 90 × 6.0	79.90	87.09	1.09	79.60	1.00
300 × 90 × 6.0	92.89	109.2	1.18	97.68	1.05
Average			1.03		0.99
COV			0.09		0.04

Note: MS- Mass scaling.

bearing lengths of 100 and 150 mm. Hence these current interaction equations can be used to predict the capacity of channel sections under combined web crippling and bending actions conservatively for bearing lengths of 50, 100 and 150 mm. However, their predictions are uneconomical for bearing lengths of 100 and 150 mm. Also, these combined web crippling-bending interaction equations only check the conservative behaviour qualitatively under combined web crippling-bending action and do not predict the accurate ultimate capacities of channel sections for a given span length. Therefore the effects of various parameters such as span length, section thickness, inside bent radius, material yield strength and bearing length on the capacity of channel

sections were investigated. In addition, a new combined web crippling-bending design equation was developed in terms of web crippling and bending capacities, span and bearing lengths, thickness and inside bent radius. The following sections describe the effect of these parameters on the capacity under combined web crippling and bending action and the development of a new design equation.

6. Effects of different parameters

6.1. Span length

The span length of channel section FE models was considered based on Zhao and Hancock's [27] equation (Equation (7)), which is based on the web crippling and bending capacities of the considered channel section and four different k factors (0.50, 0.75, 1.00 and 1.25). The ultimate failure load and moment capacities obtained from FEA for different k values were plotted as M/M_n versus P/P_n curves in Fig. 15, where M and P are the bending moment and the load at failure under combined web crippling and bending actions and M_n and P_n are their moment and web crippling capacities, all of which were obtained from FEA. In Fig. 15, k is the factor that determines the interaction relationship between moment and concentrated load. According to Equation (7), the factor k can be defined in terms of web crippling and bending capacities and span length as shown by Equation (8). The combined web crippling-bending capacities appear to plot along straight lines for k values of 0.50, 0.75, 1.00 and 1.25. Such similar variations with different k values could be used to develop a new design capacity equation.

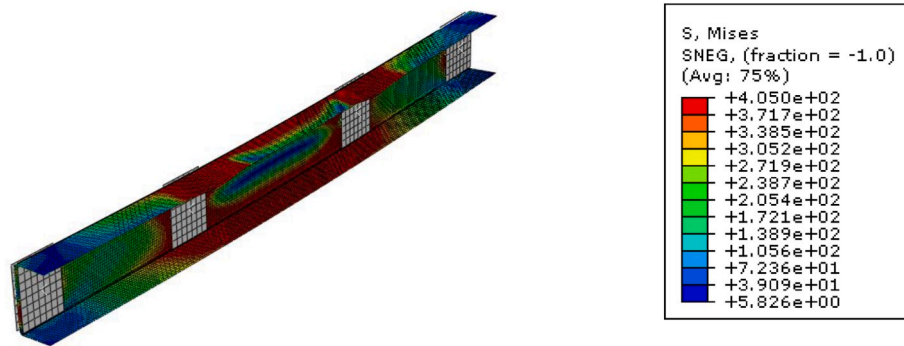
$$k = \frac{P_n L}{4M_n} \tag{8}$$

6.2. Section thickness

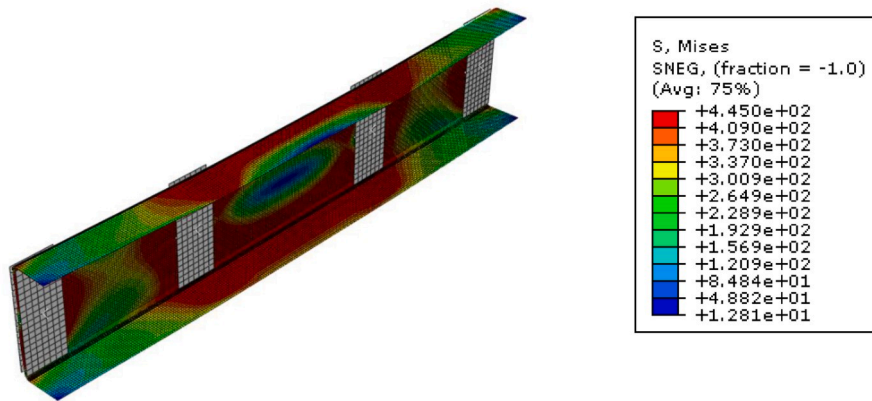
The effect of section thickness on the combined web crippling-bending interaction capacity was investigated using the channel section FE model with a depth of 200 mm, outer flange width of 75 mm and inside bent radius of 4 mm (200 × 75 mm channel). Three different section thicknesses of 1.5, 2.4 and 5.0 mm were considered with a bearing length of 100 mm. Fig. 16 shows that the combined web crippling-bending capacity of channel sections increases with section thickness.

6.3. Inside bent radius

The inside bent radius of channel sections is one of the important parameters in the web crippling capacity equations. Its effect on the web crippling and combined web crippling-bending capacity was investigated using 180 × 75 × 5 mm channel sections with different inside bent radius values of 0, 1, 4 and 10 mm for a bearing length of 150 mm. In this



(a) 125×65×4 mm channel



(b) 250×90×6 mm channel

Fig. 12. Failure modes of unlippped channels in bending with von Mises stress distribution.

Table 7

Combined web crippling and bending capacities for bearing length of 50 mm.

Section	Yield strength $f_y = 450$ MPa								Yield strength $f_y = 250$ MPa							
	Concentrated load P (kN)				Bending moment M (kNm)				Concentrated load P (kN)				Bending moment M (kNm)			
	k0.5	k0.75	k1.0	k1.25	k0.5	k0.75	k1.0	k1.25	k0.5	k0.75	k1.0	k1.25	k0.5	k0.75	k1.0	k1.25
100 × 51 × 1.5	10.5	8.3	7.9	6.9	1.6	1.8	2.3	2.5	6.8	5.3	5.1	4.3	1.0	1.2	1.5	1.5
100 × 50 × 4.0	56.3	51.4	45.4	40.6	6.1	8.0	9.3	10.2	35.0	31.7	28.4	25.2	3.6	4.7	5.5	6.0
125 × 65 × 4.0	55.9	50.8	46.1	42.0	9.1	12.1	14.4	16.2	34.6	31.1	28.7	24.3	5.2	6.8	8.3	8.7
150 × 64 × 1.5	10.3	8.4	7.9	6.9	2.3	2.8	3.5	3.8	6.7	5.4	5.1	4.2	1.6	1.9	2.3	2.4
150 × 75 × 5.0	87.0	78.3	70.9	61.5	16.3	21.5	25.6	27.6	52.8	47.7	43.0	38.8	9.3	12.3	14.6	16.3
180 × 75 × 5.0	*	77.8	70.3	61.8	*	26.5	31.6	34.5	53.1	47.2	43.1	39.0	11.5	15.1	18.2	20.4
200 × 76 × 1.5	10.2	8.7	8.2	6.9	3.3	4.1	5.2	5.4	6.6	5.4	5.0	4.5	2.3	2.8	3.5	3.9
200 × 76 × 2.4	22.8	19.8	17.8	16.4	7.4	9.5	11.4	13.0	14.7	13.1	11.6	10.7	4.8	6.3	7.4	8.5
200 × 75 × 5.0	87.5	79.1	71.6	62.0	23.0	30.6	36.7	39.5	52.9	47.3	43.0	35.0	13.0	17.2	20.7	24.4
230 × 75 × 6.0	127.4	109.2	94.8	85.3	32.6	41.2	47.3	52.9	76.7	65.4	56.4	51.0	19.6	24.7	28.1	31.7
250 × 90 × 6.0	129.0	108.2	96.1	87.9	38.1	47.2	55.5	63.2	79.6	66.3	58.3	53.0	22.7	28.0	32.5	36.8
300 × 90 × 6.0	130.5	108.0	94.2	87.6	48.1	59.0	68.3	79.1	80.5	67.0	59.4	54.2	28.4	35.0	41.1	46.7

Note: *- Specimen length is less than $3d+3l_b$ (length of web crippling specimen), where d is the overall depth and l_b is the bearing length.

case, the web crippling capacity of channel sections reduced by 48% when the inside bent radius varied from 0 to 10 mm. The combined web crippling-bending capacities of channel sections also reduced with increasing inside bent radius as shown in Fig. 17.

6.4. Material yield strength

The current combined web crippling-bending interaction design equations are based on the ratios of applied bending moment to bending capacity and applied web crippling load to web crippling capacity. Hence it is unlikely the material yield strength will affect the web crippling-bending interaction capacity equation. However, its effect was

investigated for $200 \times 76 \times 2.4$ mm unlippped channel section FE models with two different yield strengths of 250 and 450 MPa. The results shown in Fig. 18 confirm that the effect of different material yield strengths on the web crippling-bending interaction capacity equation is insignificant.

6.5. Bearing length

The effect of bearing length on the combined web crippling and bending capacity was investigated using $200 \times 76 \times 1.5$ mm channel section FE models with bearing lengths of 50, 100 and 150 mm. As expected, Fig. 19 shows that the combined web crippling-bending

Table 8
Combined web crippling and bending capacities for bearing length of 100 mm.

Section	Yield strength $f_y = 450$ MPa								Yield strength $f_y = 250$ MPa							
	Concentrated load P (kN)				Bending moment M (kNm)				Concentrated load P (kN)				Bending moment M (kNm)			
	k0.5	k0.75	k1	k1.25	k0.5	k0.75	k1	k1.25	k0.5	k0.75	k1	k1.25	k0.5	k0.75	k1	k1.25
100 × 51 × 1.5	13.8	11.9	10.4	8.9	1.9	2.3	2.6	2.8	8.3	7.9	7.5	5.6	1.2	1.6	2.0	1.8
100 × 50 × 4.0	*	74.8	66.4	55.6	*	10.2	11.6	11.8	*	45.5	40.7	34.9	*	6.0	6.8	7.0
125 × 65 × 4.0	78.2	73.5	64.9	54.3	10.7	14.1	16.1	16.5	47.7	44.6	40.4	34.2	6.2	8.3	9.7	10.1
150 × 64 × 1.5	13.6	11.5	10.4	8.9	2.8	3.4	4.1	4.3	8.0	7.4	6.5	5.6	1.8	2.4	2.8	3.0
150 × 75 × 5.0	117.0	110.7	98.3	83.4	18.3	24.6	28.4	29.5	70.0	66.2	60.4	52.2	10.7	14.4	17.0	18.1
180 × 75 × 5.0	*	108.0	93.4	79.0	*	30.6	34.5	36.0	69.4	65.3	58.5	50.4	13.4	18.1	21.1	22.4
200 × 76 × 1.5	13.5	11.7	10.2	8.9	3.7	4.7	5.4	5.8	8.1	7.2	6.1	5.2	2.6	3.4	3.8	4.0
200 × 76 × 2.4	31.7	27.7	24.4	20.0	8.4	10.7	12.3	12.5	19.6	19.6	15.2	13.2	5.5	8.1	8.2	8.8
200 × 75 × 5.0	115.6	106.8	93.1	79.2	25.5	34.1	38.8	40.8	69.3	65.3	58.8	41.4	14.7	20.0	23.5	25.9
230 × 75 × 6.0	167.6	155.7	140.2	122.4	38.3	51.5	60.6	65.4	99.9	92.8	84.6	74.1	22.9	30.7	36.6	39.6
250 × 90 × 6.0	145.5	132.5	119.9	104.6	42.5	56.4	67.0	72.4	89.5	80.5	73.6	65.9	25.2	33.0	39.6	43.9
300 × 90 × 6.0	145.2	131.9	117.5	103.0	52.0	69.2	81.2	88.4	89.5	80.4	73.5	65.7	30.9	40.6	53.5	54.1

Note: * - Specimen length is less than $3d+3l_b$ (length of web crippling specimen), where d is the overall depth and l_b is the bearing length.

Table 9
Combined web crippling and bending capacities for bearing length of 150 mm.

Section	Yield strength $f_y = 450$ MPa								Yield strength $f_y = 250$ MPa							
	Concentrated load P (kN)				Bending moment M (kNm)				Concentrated load P (kN)				Bending moment M (kNm)			
	k0.5	k0.75	k1	k1.25	k0.5	k0.75	k1	k1.25	k0.5	k0.75	k1	k1.25	k0.5	k0.75	k1	k1.25
100 × 51 × 1.5	*	15.1	13.0	11.0	*	2.9	3.1	3.2	*	9.9	8.7	7.5	*	1.9	2.1	2.1
125 × 65 × 4.0	*	91.7	77.5	63.6	*	12.6	18.4	18.3	62.0	58.5	50.6	42.4	8.1	10.3	11.3	11.4
150 × 64 × 1.5	16.0	15.1	13.0	10.9	3.2	4.3	4.7	4.9	10.2	9.1	7.7	7.4	2.1	2.7	2.9	3.5
150 × 75 × 5.0	*	140.5	121.5	101.3	*	29.0	31.9	32.3	*	85.4	76.4	64.6	*	16.9	19.3	19.7
180 × 75 × 5.0	*	136.0	117.2	100.3	*	34.1	37.7	39.4	*	84.1	75.0	63.7	*	20.2	23.1	24.0
200 × 76 × 1.5	15.0	13.8	12.0	10.0	4.0	5.3	5.7	6.1	10.1	8.9	7.6	6.4	2.9	3.7	4.0	4.2
200 × 76 × 2.4	38.6	33.4	28.4	24.2	9.7	11.9	13.2	13.8	24.4	22.0	18.8	16.5	6.1	7.8	8.7	9.3
200 × 75 × 5.0	*	133.8	115.0	98.2	*	37.5	41.5	43.4	87.5	83.4	74.0	45.3	16.8	22.5	25.7	27.3
230 × 75 × 6.0	207.4	193.3	171.0	148.2	43.7	57.5	65.7	69.7	123.2	116.7	104.6	89.9	26.0	34.7	40.2	42.3
250 × 90 × 6.0	177.4	165.0	145.1	125.6	45.5	61.4	70.8	75.8	105.5	99.9	90.3	79.0	26.6	36.6	43.3	46.9
300 × 90 × 6.0	175.1	158.9	139.8	121.9	57.3	75.1	86.4	92.9	103.9	97.5	87.8	77.0	33.6	45.5	53.5	57.9

Note: * - Specimen length is less than $3d+3l_b$ (length of web crippling specimen), where d is the overall depth and l_b is the bearing length.

capacities of channel section increases with increasing bearing length.

7. Improvements to the current web crippling-bending interaction equation

The current combined web crippling and bending interaction design equations in the cold-formed steel standards are based on the relationship between the ratios of applied bending moment to bending capacity and applied web crippling load to web crippling capacity. Last section presented the effects of various parameters on the combined web crippling-bending capacities compared to the current web crippling-bending interaction equations. As expected, the variation of combined web crippling-bending capacities of channel sections was linear for different k values of 0.50, 0.75, 1.00 and 1.25 as shown in Fig. 15. The linear gradient ratio of line k0.75 to line k0.50 is approximately equal to the ratio of k values ($0.75/0.50 = 1.5$) and a similar pattern was observed for other k values. The k value depends on the pure web crippling and bending capacities of channel sections, and the span length (Equation (8)). All the lines obtained for the k values of 0.75, 1.00 and 1.25 were moved to the line for the k value of 0.50 by incorporating $\sqrt{2k}$ with the load value (P) on the x-axis and $\sqrt{2k}$ with the bending moment capacity (M_n) on the y-axis as shown in Fig. 20.

After the above modification in Fig. 20, one of the following conditions (Equations (9) and (10)) should be satisfied for the safe design of channel sections subject to combined web crippling-bending actions.

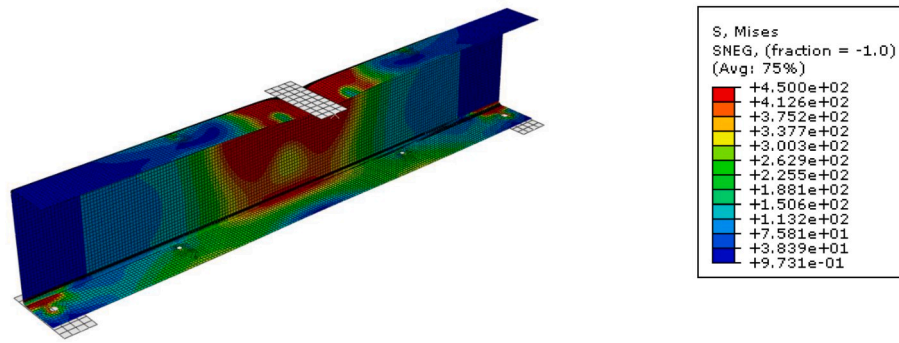
$$P\sqrt{2k}/P_n \leq 0.8 \tag{9}$$

$$M/\sqrt{2k}M_n \leq 0.4 \tag{10}$$

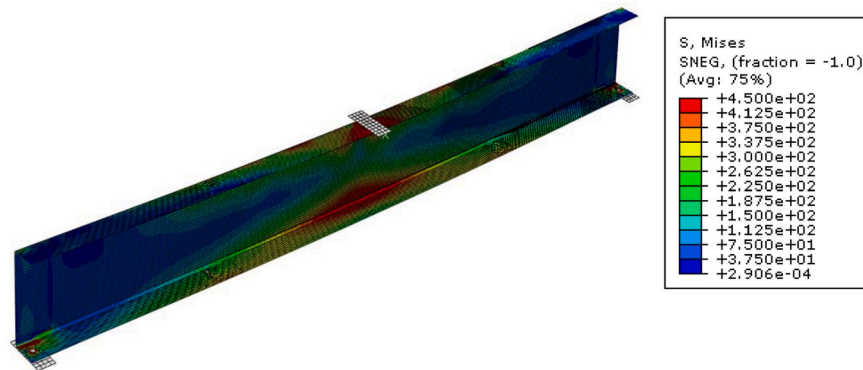
However, the effect of inside bent radius and bearing lengths were not included in this modification. Therefore a new design equation which includes the effects of inside bent radius and bearing length was developed and proposed next. The proposed equation can be used to determine the design strength of channel sections subject to combined web crippling and bending actions.

7.1. Proposed design equation

The combined web crippling-bending capacities of unlippped channel sections with varying bearing and span lengths as obtained from FEA (Tables 7–9) are compared with the combined web crippling-bending capacity equations in the current cold-formed steel design standards in Fig. 14. It shows a significant inconsistency (underestimation for bearing lengths of 100 and 150 mm) by these design interaction equations for the G250 and G450 unlippped channel sections considered in this study. The detailed FEA study was conducted to determine the effects of various parameters as discussed in Section 6. Similar variation was observed for the combined web crippling and bending capacities of unlippped channel sections with span length (L), which was chosen based on different k values (0.50, 0.75, 1.00 and 1.25). Equations (9) and (10) were developed based on the FEA results shown in Fig. 20. In both Equations (9) and (10), one of the following conditions should be satisfied for the safe design of unlippped channel sections under combined web crippling and bending actions. The applied load (P) should be less than $0.8P_n/\sqrt{2k}$ based on Equation (9), in which the k value can be



(a) Short span ($k = 0.5$)



(b) Long span ($k = 1.25$)

Fig. 13. Comparison of web crippling-bending failure modes for $k = 0.5$ and 1.25 with von Mises stress distribution.

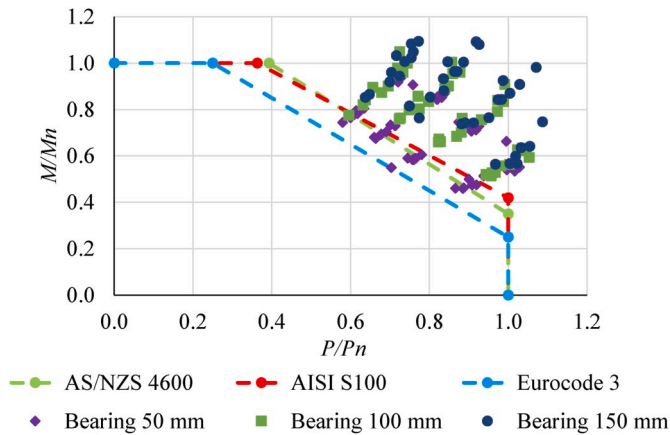


Fig. 14. Comparison of FEA capacities with current design equations for combined web crippling and bending actions.

replaced by $\frac{P_n L}{4M_n}$ based on Equation (8). Therefore, Equation (11) should be satisfied for the safe design of unlippped channel sections under combined web crippling and bending actions.

$$P \leq 0.8 \sqrt{\frac{2M_n P_n}{L}} \quad (11)$$

The effects of bearing length and inside bent radius were obtained from FEA and were incorporated within Equation (11) as shown in Equation (12). Equation (12) can be used to accurately determine the combined web crippling-bending capacity of unlippped channel sections, ie. the mid-span concentrated load capacity (P) under combined web crippling and bending actions, for bearing lengths greater than 50 mm.

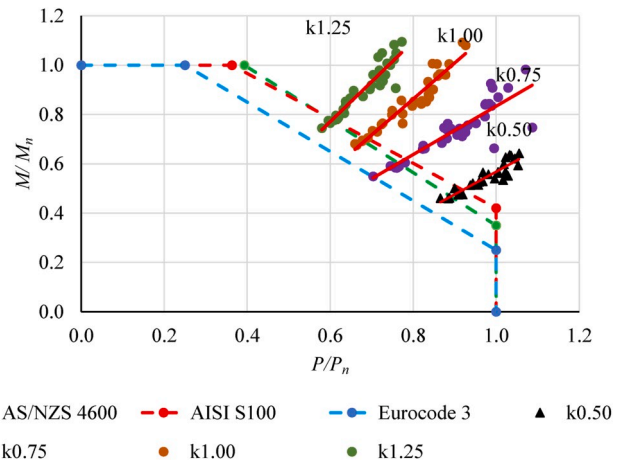


Fig. 15. Effect of span length on the combined web crippling-bending capacities of channel sections.

$$P = \sqrt{\frac{2(1 + \alpha l_b) M_n P_n}{L}} \left(1 - 0.1 \sqrt{\frac{r_i}{t}} \right) \quad (12)$$

for span length $L > 3d + 2l_b$, where d - depth of channel section ($100 < d < 300$ mm), l_b - bearing length, r_i - inside bent radius ($1 < r_i < 10$ mm), t - thickness of channel sections ($1.5 < t < 6$ mm) and f_y - yield strength of channel section in MPa (250 and 450). The bending (M_n) and web crippling (P_n) capacities of channel sections were obtained from FEA for the calibration of this equation. The coefficient (α) is equal to 0.006/mm. Equations (11) and (12) are applicable only to beams subject to a mid-span concentrated load.

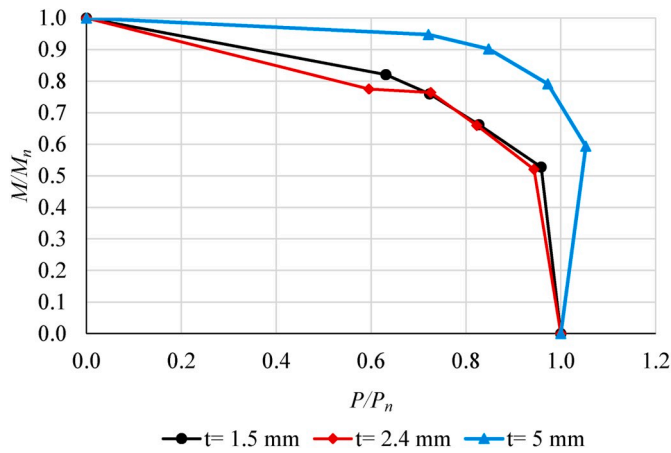


Fig. 16. Effect of section thickness on the combined web crippling-bending capacities of channel sections.

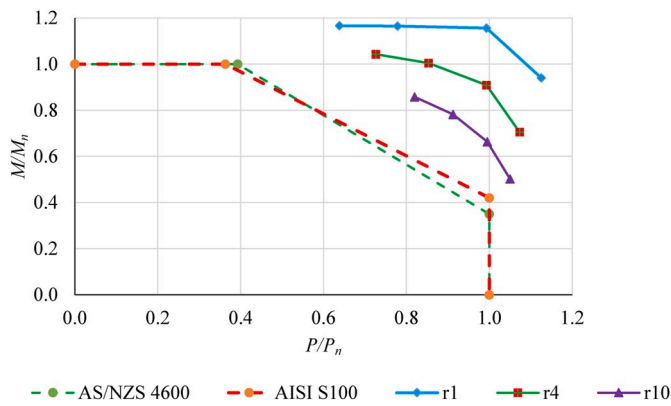


Fig. 17. Effect of inside corner radius on the combined web crippling-bending capacities of channel sections.

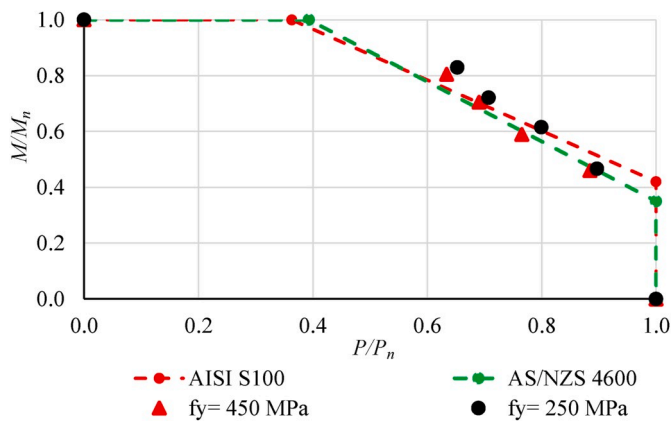


Fig. 18. Effect of material yield strength on the combined web crippling-bending capacities of channel sections.

Fig. 21 shows the comparison of combined web crippling-bending capacities obtained from FEA and the proposed equation. Equation (12) predicted the combined web crippling-bending capacities of most of the considered G450 and G250 channel sections within an error margin of -10% to $+10\%$ with a few values within an error margin of -15% to $+15\%$. The overall mean and COV values of combined web crippling-bending capacities obtained from FEA to predicted values using the proposed equation is 1.015 and 0.063, respectively. Therefore, Equation

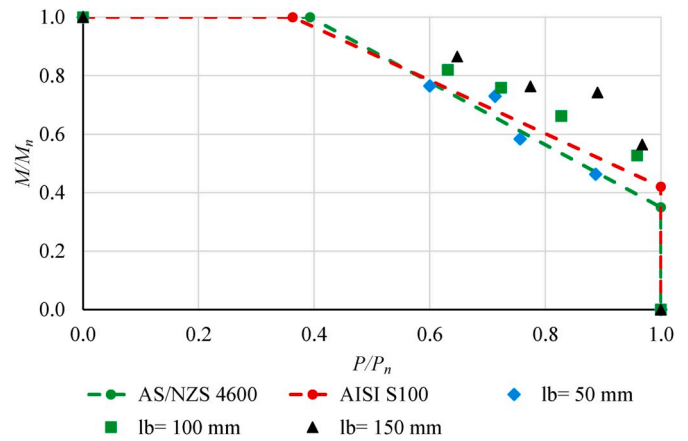


Fig. 19. Effect of bearing length on the combined web crippling-bending capacities of channel sections.

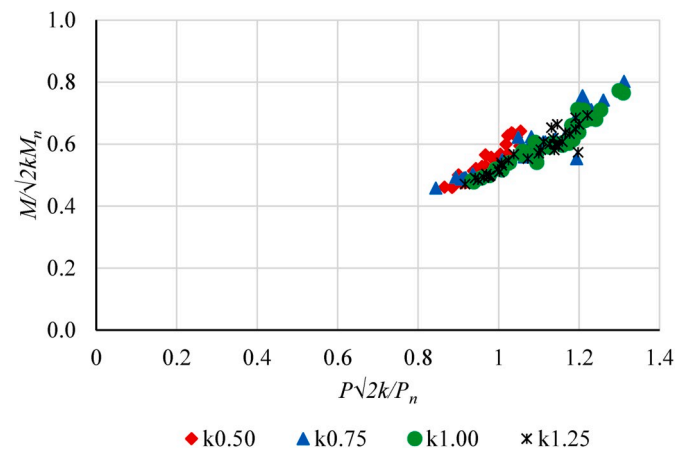


Fig. 20. Modification to the current web crippling-bending interaction equation.

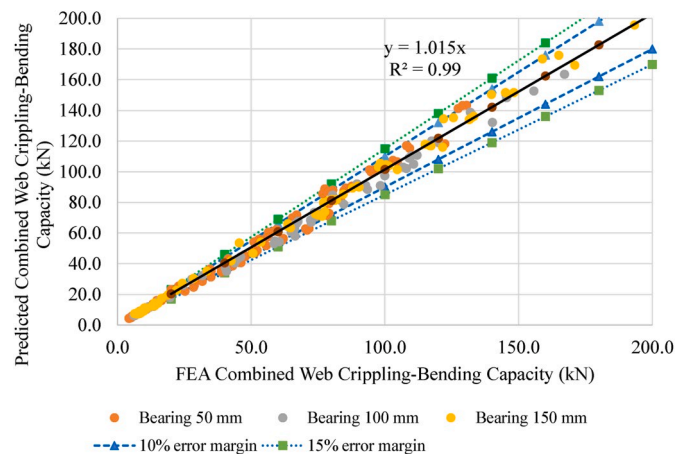


Fig. 21. Comparison of combined web crippling and bending capacities obtained using the proposed design equation and FEA.

(12) can be used to predict the design capacity of channel sections subject to combined web crippling and bending actions.

7.2. Capacity reduction factor

A suitable capacity reduction factor is required to determine the

design combined web crippling-bending capacity using the proposed design equation (Equation (12)). The North American specification AISI S100 [4] recommends the following equation to calculate the capacity reduction factor (ϕ_w).

$$\phi_w = CM_m F_m P_m e^{-x} \quad (13)$$

where $x = \beta_0 \sqrt{V_M^2 + V_F^2 + C_p V_P^2 + V_Q^2}$

In Equation 13, C is equal to 1.521 from AISI S100. The statistical parameters are obtained from Table F1 of AISI S100 for combined web crippling and bending strength, where $M_m = 1.1$, $F_m = 1.0$, $V_M = 0.1$ and $V_F = 0.05$. The parameters P_m and V_p are the mean and the coefficient of variation of the tested to predicted load ratio. The statistical parameter V_Q is the coefficient of variation of load effects and depends on the dead load to live load ratio (D/L). It is given as 0.21 in AISI S100. The parameter C_p is a correction factor for small number of tests and is given by $\left[1 + \frac{1}{n}\right] \left[\frac{m}{m-2}\right]$; n is number of tests; m is degree of freedom = $n - 1$. The values of P_m and V_p in this case (combined web crippling-bending capacity) are 1.01 and 0.063, which are based on the ratios of all the capacities from FEA and proposed design equation. Using these values, Equation (13) gives a capacity reduction (ϕ_w) of 0.90 for a target reliability index β_0 of 2.5.

8. Conclusions

This paper has presented the details and results of a finite element analysis based investigation into the combined web crippling-bending interaction behaviour of cold-formed steel channel sections used as bearers in floor systems with fastened supports. Finite element models developed and validated by the authors in a recent web crippling study [15] were extended to investigate the behaviour of unlippped channel sections subject to combined action of web crippling and bending while new finite element models of unlippped channel sections in bending were developed and validated using Young and Hancock's (10) test results. Validated finite element models were then used in a detailed numerical parametric study of 12 unlippped channels made of two steel grades (G250 and G450) to investigate the interaction behaviour and obtain a large capacity data base for combined web-crippling and bending action. Three types of finite element models were used to obtain the capacities of unlippped channel sections under pure and combined web crippling and bending actions. In the parametric study, the span lengths of web crippling-bending interaction finite element models were chosen based on an equation proposed by Zhao and Young [27].

Comparison of the capacities of unlippped channels under combined web crippling and bending actions obtained from finite element analyses with those predicted by the currently used interaction equations in three cold-formed steel design standards, AISI S100, AS/NZS 4600 and Eurocode 3 Part 1.3, showed that the current design equations are accurate for 50 mm bearing length. However, they can also be used to predict the combined web crippling-bending capacities conservatively for bearing lengths of 100 and 150 mm. A new design equation with a suitable capacity reduction factor was proposed to improve the accuracy of predicting the mid-span load capacity of channel sections subject to combined web crippling and bending actions.

CRediT authorship contribution statement

Balasubramaniam Janarthanan: Conceptualization, Methodology, Investigation, Formal analysis, Validation, Data curation, Writing - original draft. **Mahen Mahendran:** Conceptualization, Validation, Supervision, Writing - review & editing, Resources, Project administration, Funding acquisition.

Acknowledgements

The authors would like to thank Australian Research Council and Austube Mills for their financial support (Grant Number LP120200650) and QUT for providing the necessary facilities and support to this project. They would also like to thank Dr Shanmuganathan Gunalan for his guidance in the early stages of the first author's PhD research.

References

- [1] Onesteel Market Mills, Duragal Design Capacity Tables for Structural Steels Angles, Channels and Flats, 2001. Brisbane, Australia.
- [2] American Iron and Steel Institute (AISI), Standard Test Method for Determining the Web Crippling Strength of Cold-Formed Steel Beams, 2013. TS-9-05, Washington DC, USA.
- [3] W.W. Yu, Cold-formed Steel Design, John Wiley & Sons, Inc, 2000.
- [4] American Iron and Steel Institute (AISI), North American Specification for the Design of Cold-Formed Steel Structural Members AISI S100, 2012. Washington, DC, USA.
- [5] Standards Australia, Cold-formed Steel Structures, 2018. AS/NZS 4600, Sydney, Australia.
- [6] European Committee for Standardization (ECS), Eurocode 3 Part 1.3, Design of Steel Structures: Part 1.3: General Rules - Supplementary Rules for Cold-Formed Thin Gauge Members and Sheeting, European Committee for Standardization, Brussels, Belgium, 2006.
- [7] R. Baehre, Sheet Metal Panels for Use in Building Construction - Recent Research Projects in Sweden, Proceeding of the Third International Specialty Conference on Cold-Formed Steel Structures, University of Missouri-Rolla, Rolla, Missouri, USA, 1975.
- [8] G.D. Ratliff, Interaction of concentrated loads and bending in C-shaped beams, in: Proceedings of the Third Specialty Conference on Cold-Formed Steel Structures, University of Missouri-Rolla, Rolla, Missouri, USA, 1975.
- [9] N. Hetrakul, W.W. Yu, Structural Behaviour of Beam Webs Subjected to Web Crippling and a Combination of Web Crippling and Bending, Final Report, Civil Engineering Study 78-4, University of Missouri-Rolla, Rolla, Missouri, USA, 1978.
- [10] B. Young, G. Hancock, Tests of channels to combined bending and web crippling, J. Struct. Eng. 128 (2002) 300-308.
- [11] S. Gunalan, M. Mahendran, Experimental study of unlippped channel beams subject to web crippling under one flange load cases, Advanced Steel Construction 15 (2) (2019) 165-172.
- [12] B. Janarthanan, M. Mahendran, S. Gunalan, Bearing capacity of cold-formed unlippped channels with restrained flanges under EOF and IOF load cases, Steel Construction 3 (2015) 146-154.
- [13] P. Keerthan, M. Mahendran, E. Steau, Experimental study of web crippling behaviour of hollow flange channel beams under two flange load cases, Thin-Walled Struct. 85 (2014) 207-219.
- [14] E. Steau, P. Keerthan, M. Mahendran, Web crippling study of rivet fastened rectangular hollow flange channel beams with flanges fastened to supports, Adv. Struct. Eng. 20 (7) (2017) 1059-1073.
- [15] B. Janarthanan, M. Mahendran, S. Gunalan, Numerical modelling of web crippling failures in cold-formed steel unlippped channel sections, J. Constr. Steel Res. 158 (2018) 486-501.
- [16] W. Ren, S. Fang, B. Young, Analysis and design of cold-formed steel channels subjected to combined bending and web Crippling, Thin-Walled Struct. 44 (2006) 314-320.
- [17] American Iron and Steel Institute (AISI), North American Specification for the Design of Cold-Formed Steel Structural Members AISI S100, 2001. Washington DC, USA.
- [18] M.S. Soliman, A.B.B. Abu-Sena, E.E.H. Darwish, M.S.R. Saleh, Resistance of cold-formed steel sections to combined bending and web crippling, Ain Shams Eng. J. 4 (2013) 435-453.
- [19] American Iron and Steel Institute (AISI), North American Specification for the Design of Cold-Formed Steel Structural Members AISI S100, 2007. Washington DC, USA.
- [20] Standards Australia, Cold-formed Steel Structures, 1996. AS/NZS 4600, Sydney, Australia.
- [21] British Standards Institution, Structural Use of Steelwork in Building: Part 5, Code of Practice for Design of Cold-Formed Sections BS5950, 1998. London, UK.
- [22] Ministerial Decree, Egyptian Code of Practice for Steel Construction (ECP-LRFD) Load and Resistance Factor Design, 2007. Cairo, Egypt.
- [23] Standards Australia, Methods for Tensile Testing of Metal AS 1391, 2007. Sydney, Australia.
- [24] ABAQUS Version 6.14, Analysis User's Guide, Dassault Systems Simulia Corp, Providence, RI, USA.
- [25] ABAQUS Version 6.14, Theory Guide, Dassault Systems Simulia Corp, Providence, RI, USA.
- [26] P. Nataro, N. Silvestre, D. Camotim, Web crippling failure using quasi-static FE Models, Thin-Walled Struct. 84 (2014) 34-49.
- [27] X.L. Zhao, G.J. Hancock, Square and rectangular hollow section under transverse end-bearing force, J. Struct. Eng. 121 (1995) 1323-1329.